



# Structures and Field Emission Properties of Silicon Nanowire Arrays Implanted with Energetic Carbon Ion Beam

Guo-An Cheng\*, Fei Zhao, Shao-Long Wu, Dan-Dan Zhao,  
Jian-Hua Deng, Rui-Ting Zheng, and Zhao-Xia Ping

Key Laboratory of Beam Technology and Material Modification of Ministry of Education,  
College of Nuclear Science and Technology, Beijing Normal University, Beijing 100875, China

Structures and field emission properties of silicon nanowire arrays (SiNWAs), which were fabricated by using of electroless-chemical etching method and post-implanted by the energetic carbon ion beam with an average energy of 20 keV at various doses, have been investigated. Structural analysis of SEM and XPS shows that SiC compound had been formed at the top of SiNWAs, and Si-C/Si composite nanostructure had been obtained. Compared to as-grown SiNWAs, the C ion implanted SiNWAs have better field emission characteristics. The turn-on field and the applied field at  $100 \mu\text{A}/\text{cm}^2$  are reduced from 5.01 V/ $\mu\text{m}$  and 5.93 V/ $\mu\text{m}$  for as-grown SiNWAs to 4.45 V/ $\mu\text{m}$  and 5.40 V/ $\mu\text{m}$  for SiNWAs implanted at the dose of  $1 \times 10^{16} \text{ cm}^{-2}$ , respectively. However, large implanting amounts made serious structural damages at the top of nanowires, and impaired the field emission characteristics. The influence of energetic C ion implantation on the structures and field emission properties of SiNWAs has been discussed.

## Keywords:

## 1. INTRODUCTION

In the last decades, SiNWAs have attracted a great deal of attention due to their one-dimensional nanostructure and size-dependent physical properties, which are promising for applications in the field emission display (FED),<sup>1</sup> photovoltaics,<sup>2</sup> biosensors,<sup>3</sup> chemical sensors,<sup>4</sup> gas sensors,<sup>5</sup> photo-detectors<sup>6</sup> and future nanoscale devices. There are many kinds of methods to fabricate silicon nanowires, such as laser ablation,<sup>7</sup> oxide-assisted growth (OAG),<sup>8</sup> thermal evaporation,<sup>9</sup> chemical vapor deposition (CVD)<sup>10</sup> and electroless-chemical etching method (EED).<sup>11-12</sup> Recently, a great amount of researches have been done to modify silicon nanowires to get better properties, including doping,<sup>13-15</sup> surface decoration of nanowires<sup>16-17</sup> and post-annealing,<sup>18</sup> etc. Ion implantation into silicon materials, especially into thin film materials,<sup>19-20</sup> has been a long practice to modify the field emission properties by controlling various dopants with different doses. Reports demonstrate that the field emission characteristics of the ion implanted Si nanostructure have been greatly improved due to the formation

of SiC/Si heterostructure.<sup>21</sup> However, there is a little study on ion implantation to the well aligned SiNW arrays and their FE properties.

In this paper, the structures and field emission properties of energetic C ion implanted SiNWAs were investigated, and the influence of ion implantation on structures and properties was discussed.

## 2. EXPERIMENTAL DETAILS

Vertically aligned SiNWAs based on *N* type (100) silicon wafer with resistivity of  $7 \sim 10 \Omega \cdot \text{cm}$  were *in-situ* fabricated by using a relative simple approach, which is similar to our previous reported technology.<sup>11, 12</sup> The process mainly included three steps: (1) cleaning of original silicon wafers; (2) immersion of the cleaned silicon wafers into HF-based aqueous solution containing silver nitrate to synthesize Ag nano-catalyst; (3) etching the Ag nano-catalyst covered silicon by immersing them into HF-base aqueous solution containing oxidant ( $\text{H}_2\text{O}_2$  or  $\text{Fe}(\text{NO}_3)_3$ ). After above processes, the surface colour of samples turned to black, and then the samples were immersed into 50%  $\text{HNO}_3$  boiled-solution to dissolve Ag nano-catalyst.

\* Author to whom correspondence should be addressed.

As-grown SiNWAs were implanted by energetic carbon ion with an average energy of 20 keV at room temperature using a metal vapor vacuum arc ion source. The implanted dose was in the range from  $1 \times 10^{16}$  to  $5 \times 10^{17} \text{ cm}^{-2}$ . Field emission scanning electron microscopy (SEM Hitachi S-4800) was employed to characterize the morphology of as-grown SiNWAs and the carbon ion-implanted samples with different doses. The C concentration depth profile in the as-implanted SiNWAs was analyzed by the scanning energy-dispersive X-ray spectroscopy (EDX), and X-ray photoelectron spectroscopy (XPS) was used to characterize the chemical bonding state of Si and C in the SiNWAs. The field emission measurements were carried out in an ultrahigh vacuum chamber, in which the working voltage ranged from 0 to 10 kV was supplied and the data was automatically recorded by a computer connected to the measurement system. The distance between the anode and cathode was varied from 0 to 5000  $\mu\text{m}$  and controlled by an electric manipulator.

### 3. RESULTS AND DISCUSSION

Typically, microstructures of as-grown SiNWAs and the ion-implanted SiNWAs by energetic carbon ion with an average energy of 20 keV at various doses are shown in Figure 1. From Figure 1, it can be seen that morphologies of the ion-implanted SiNWAs at doses of  $1 \times 10^{16}$  and  $5 \times 10^{16} \text{ cm}^{-2}$  are almost similar as that of as-grown SiNWAs (seen Figs. 1(a, b and e)). However, for the ion-implanted SiNWAs at a dose above  $5 \times 10^{16} \text{ cm}^{-2}$ , obvious changes on the surface microstructures are observed at the ion-implanted SiNWAs, in which the porous and fine-spiculate structures at the tips of SiNWAs gradually disappeared due to the effect of energetic ion sputtering during ion implantation, and transformed to smooth tips at the ion-implanted SiNWAs with a dose of  $5 \times 10^{17} \text{ cm}^{-2}$ . Herein, the C ion beam implantation has an important impact on the structures of as-grown SiNWAs, and more damages will be introduced to SiNWAs with an increasing

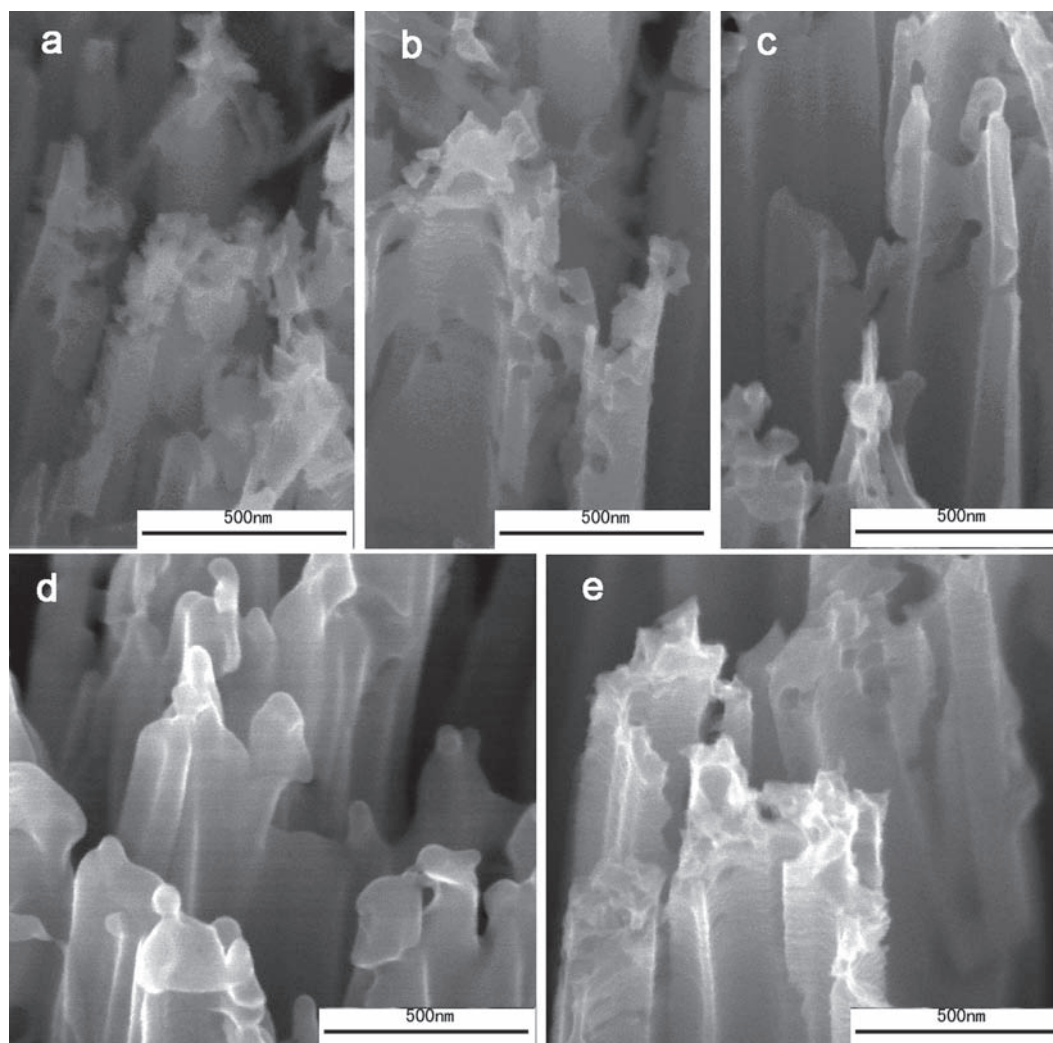


**Fig. 1.** SEM images of the implanted SiNWAs with C dose of  $1 \times 10^{16} \text{ cm}^{-2}$  (a)  $5 \times 10^{16} \text{ cm}^{-2}$  (b)  $1 \times 10^{17} \text{ cm}^{-2}$  (c)  $5 \times 10^{17} \text{ cm}^{-2}$  (d) and as-grown SiNWAs (e).

dose. On the other hand, the C depth profile measured by EDX in the implanted SiNWAs at a dose of  $1 \times 10^{16} \text{ cm}^{-2}$  (seen in Fig. 2) indicates that C element has been doped into the top of SiNWAs and distributes in the region from tips of the array to  $2.21 \mu\text{m}$  in depth.

In order to understand the chemical structure clearly, XPS analysis was used to determine the chemical structures of C and Si elements in the C implanted SiNWAs. Figure 3 shows C1s peaks and Si2p peaks in XPS spectra of SiNWAs. From Figure 3, it can be seen that each peak is composed of several lines, which are obtained by peak fitting with Gauss's function. Three peaks located at 283.2 eV, 284.1 eV and 285.0 eV respectively are observed in C1s peak, in which lines are corresponding to Si-C covalent band,  $\text{sp}^2$ -bond and  $\text{sp}^3$ -bond,<sup>22</sup> and the corresponding contents are 55%, 29% and 16% respectively. These indicate that 55% implanted C element was used to form Si-C compound. On the other hand there are three peaks located at 98.4 eV, 100.8 eV and 102.1 eV respectively also to be observed in Si2p peak, in which lines are corresponding to Si-Si covalent bands, Si-C covalent bands and Si-O covalent bands,<sup>22</sup> and the corresponding contents are 60%, 11% and 29% respectively. The content of Si-C covalent bands increases with the increasing C ion implantation dose. These demonstrate that SiC compound has been formed at the top of SiNWAs during energetic C ion implantation, and SiC-Si composite nanostructure/SiNW heterostructures have been synthesized via C implantation into SiNWAs.

Field electron emission characteristics of the implanted SiNWAs at various doses are shown in Figure 4. A remarkable diversification of current density versus electric field ( $J$ - $E$ ) characteristics at various doses is observed in Figure 4(a), where the curve of the SiNWAs implanted at a dose of  $1 \times 10^{16} \text{ cm}^{-2}$  moved to the low applied field. However, high dose implantation induces the curve moving to the high applied field, and makes field emission characteristics of SiNWAs worse. It illuminates that

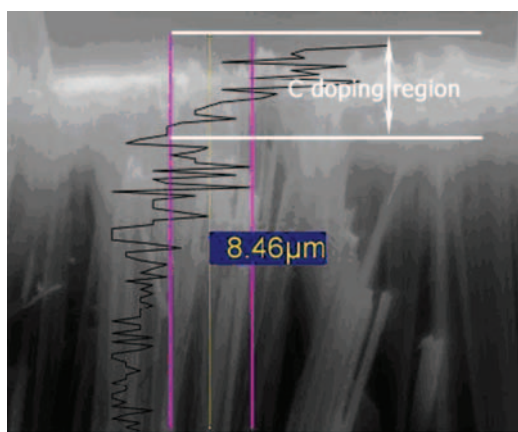


**Fig. 2.** Scanning EDX spectrum of the C element along with the depth of SiNWAs.

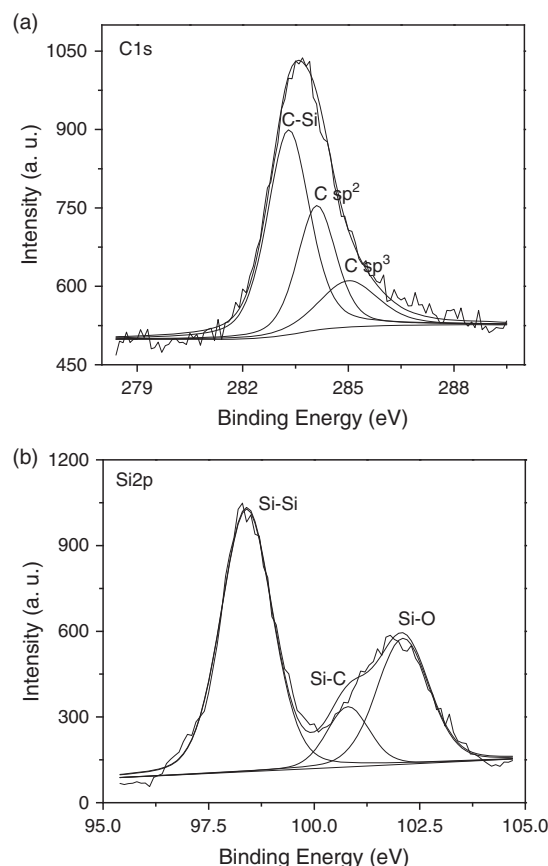


**Fig. 3.** C1s peak (a) and Si2p peak (b) in the XPS spectra of SiNWAs implanted at the dose of  $1 \times 10^{16} \text{ cm}^{-2}$ .

low dose implantation of C ions makes electron emission ease at the low applied field and enhances field emission of SiNWAs. Figure 4(b) shows the changes of turn on fields (at which the current density is  $10 \mu\text{A}/\text{cm}^2$ ) and the applied fields of SiNWAs at the current density of  $100 \mu\text{A}/\text{cm}^2$  versus ion implantation doses. The turn-on field of the implanted SiNWAs at the dose of  $1 \times 10^{16} \text{ cm}^{-2}$  is about  $4.45 \text{ V}/\mu\text{m}$ , and lower than that of as-grown SiNWAs. Similar variation tendency is also observed when the current density is  $100 \mu\text{A}/\text{cm}^2$ , in which the minimum applied field is  $5.40 \text{ V}/\mu\text{m}$  for the implanted SiNWAs at the dose of  $1 \times 10^{16} \text{ cm}^{-2}$ , and lower than that of as-grown SiNWAs ( $5.93 \text{ V}/\mu\text{m}$ ).

Fowler-Nordheim ( $F$ - $N$ ) plots of  $\ln(J/E^2)$  versus  $1/E$  are shown in the inset of Figure 4(a). Field emission characteristics of the implanted SiNWAs were analyzed by using of the Fowler-Nordheim (FN) equation given below:<sup>23</sup>

$$\ln\left(\frac{J}{E^2}\right) = \ln(ra\phi^{-1}\beta^2) - \frac{sb\phi^{3/2}\beta^{-1}}{E} \quad (1)$$

Where  $\Phi$  is the work function,  $\beta$  is the field enhancement factor,  $a$  and  $b$  are the  $F$ - $N$  constants,  $r$  and  $s$  are appropriate values of intercept and slope correction factors, respectively. According to the equation,  $F$ - $N$  plot is

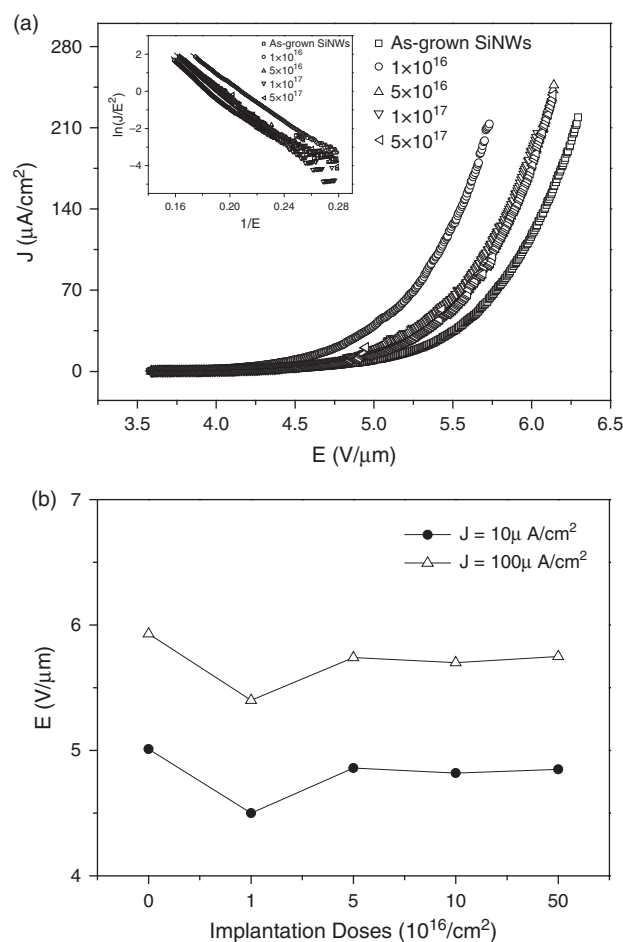


**Fig. 4.** Field emission characteristics of SiNWAs implanted at various doses. (a)  $J$ - $E$  curves, inset is the corresponding  $F$ - $N$  plots; (b) changes of turn on fields and the applied fields of SiNWAs at the current density of  $100 \mu\text{A}/\text{cm}^2$  versus ion implantation doses.

expected to be a good straight line because of small variation of  $r$  and  $s$  with  $1/E$ . Further to simplify the equation above,  $r$  multiplied by  $a$  equals to a constant of  $1.54 \times 10^{-6} \text{ A (eV)}^{-1} \text{ V}^{-2}$  and  $s$  multiplied by  $b$  equals to a constant of  $6.83 \times 10^3 \text{ (eV)}^{-3/2} \text{ V } (\mu\text{m})^{-1}$ . It has been observed that all the FN plots of SiNWAs shown in the inset of Figure 4(a) are approximate straight lines in the high current density areas and fit with the  $F$ - $N$  equation, which suggests that the electrons are emitted by the cold FE process.

Field emission characteristics associate with structures (composition, tip sharpness, aspect ratio, etc.) and electrical parameters (conductivity, work function, etc.) of emitters. Energetic ion implantation into materials leads to defect creation (substitution, interstitial and vacancy creation), doping, re-crystallization and other interesting phenomena, and makes characteristics of materials changing. During C ion implantation into SiNWAs, interaction between incident ions and Si atoms induced surface sputtering effect and structural damages in SiNWAs, and formed amount of interstitial atoms and vacancies. Surface sputtering effect

induced the porous and fine-spiculate structures at the tips of SiNWAs to be removed gradually with increasing implantation doses, and formed smooth tips finally, which reduces field enhancement effect. At lower dose implantation, changes of micro-structures at tips of SiNWAs were small, which illuminated that a similar field enhancement effect, as that of as-grown SiNWAs, might be obtained. On the other hand, structural damages induced by implantation indicated the formation of amorphous Si, which makes the energy level of Si atoms rise and reduces field enhancement effect. At the same time, as shown in XPS spectra, Si-C compound was formed due to C ion implantation. These demonstrate that Si-C/Si composite nanostructure have been synthesized after energetic C ion implantation, which reduces the work function of the emitter and makes electron emission easily. Considering on the lower irradiation damages at the dose of  $1 \times 10^{16} \text{ cm}^{-2}$ , the field emission characteristics of the implanted SiNWAs was enhanced due to the formation of Si-C/Si composite nanostructures. However, large structural damages, which reduce the amount of emitting points and field enhancement effect of SiNWAs, made the field emission characteristics of SiNWAs worsen.

#### 4. Summary

Energetic C ion implantation in SiNWAs affected the structures and field emission characteristics of SiNWAs. Low dose implantation induced the changes of micro-structures at tips of SiNWAs small. With an increasing implantation dose, the porous and fine-spiculate structures at tips of SiNWAs were removed gradually, and changed to smooth tips finally. Si-C/Si composite nanostructures based on SiNWAs have been synthesized by energetic C ion implantation. The field emission characteristics of the implanted SiNWAs alternatively changed with the increasing implantation doses. The minimum turn on field ( $4.45 \text{ V}/\mu\text{m}$ ) and the applied field ( $5.40 \text{ V}/\mu\text{m}$ ) at current density of  $100 \mu\text{A}/\text{cm}^2$  have been obtained in the implanted SiNWAs with a dose of  $1 \times 10^{16} \text{ cm}^{-2}$ , and is lower than that of as-grown SiNWAs. These demonstrate that the field emission characteristics of the implanted SiNWAs have been enhanced due to the formation of Si-C/Si composite nanostructures. High dose implantation created large structural damages, which make the field emission characteristics of SiNWAs worse. Therefore, energetic C ion beam processing SiNWAs may be a feasible way to enhance field emission characteristics of SiNWAs, and Si-C/Si composite nanostructure has a potential for application in field emission display.

**Acknowledgments:** This work is supported by the National Basic Research Program of China (No: 2010CB832905), and partially by the Key Scientific and Technological Project of Ministry of Education of China (No: 108124).



## References and Notes

1. J. Zhou, Y. Ding, S. Z. Deng, L. Gong, N. S. Xu, and Z. L. Wang, *Adv. Mater.* 17, 2107 (2005).
2. K. Q. Peng, X. Wang, X. L. Wu, and S. T. Lee, *Nano Lett.* 9, 3704 (2009).
3. G. J. Zhang, J. H. Chua, R. E. Chee, A. Agarwal, S. M. Wong, K. D. Buddharaju, and N. Balasubramanian, *Biosens. Bioelectron.* 23, 1701 (2008).
4. S. Sen, P. Kanitkar, A. Sharma, K. P. Muthe, A. Rath, S. K. Deshpanda, M. Kaur, R. C. Aiyer, S. K. Gupta, and J. V. Yakhmi, *Sens. Actuators B.* 147, 453 (2010).
5. J. Wan, S. R. Deng, R. Yang, Z. Shu, B. R. Lu, S. Q. Xie, Y. F. Chen, E. Huq, R. Liu, and X. P. Qu, *Microelectro. Eng.* 86, 1238 (2009).
6. F. Patolsky, B. P. Timko, G. H. Yu, Y. Fang, A. B. Greytak, G. F. Zheng, and C. M. Lieber, *Science* 313, 1100 (2006).
7. A. M. Morales and C. M. Lieber, *Science* 279, 208 (1998).
8. R. Q. Zhang, Y. Lifshitz, and S. T. Lee, *Adv. Mater.* 15, 635 (2003).
9. H. F. Yan, Y. J. Xing, Q. L. Hang, D. P. Yu, Y. P. Wang, J. Xu, Z. H. Xi, and S. Q. Feng, *Chem. Phys. Lett.* 323, 224 (2000).
10. Y. Y. Wong, M. Yahaya, M. M. Salleh, and B. Majlis, *Sci. Technol. Adv. Mater.* 6, 330 (2005).
11. F. Zhao, G. A. Cheng, R. T. Zheng, and L. Y. Xia, *J. Korean Phys. Soc.* 52, s104 (2008).
12. F. Zhao, D. D. Zhao, S. L. Wu, G. A. Cheng, and R. T. Zheng, *J. Korean Phys. Soc.* 55, 2681 (2009).
13. C. T. Huang, C. L. Hsin, K. W. Huang, C. Y. Lee, P. H. Yeh, U. S. Chen, and L. J. Chen, *Appl. Phys. Lett.* 91, 093133 (2007).
14. Y. W. Ok, T. Y. Seong, C. J. Choi, and K. N. Tu, *Appl. Phys. Lett.* 88, 043106 (2006).
15. Y. H. Tang, X. H. Sun, F. C. K. Au, L. S. Liao, H. Y. Peng, C. S. Lee, and T. K. Sham, *Appl. Phys. Lett.* 79, 1673 (2001).
16. T. C. Wong, C. P. Li, R. Q. Zhang, and S. T. Lee, *Appl. Phys. Lett.* 84, 407 (2004).
17. J. K. Ha, B. H. Chung, S. Y. Han, and J. O. Choi, *J. Vac. Sci. Technol. B* 20, 2080 (2002).
18. B. Q. Zeng, G. Y. Xiong, S. Cheng, S. H. Jo, W. Z. Wang, D. Z. Wang, and Z. F. Ren, *Appl. Phys. Lett.* 88, 213108 (2006).
19. Y. M. Xing, J. H. Zhang, W. W. Yang, Y. H. Yu, Z. R. Song, and Z. X. Lin, *Appl. Phys. Lett.* 84, 5461 (2004).
20. F. Y. Meng, W. K. Wong, N. G. Shang, Q. Li, and I. Bello, *Vacuum* 66, 71 (2002).
21. Y. Han, R. W. M. Kwok, and S. P. Wong, *Diamond Relat. Mater.* 5, 556 (1996).
22. H. P. Liu, G. A. Cheng, C. L. Liang, and R. T. Zheng, *Nanotechnol.* 19, 245606 (2008).
23. R. G. Forbes, *Ultramicroscopy*. 79, 11 (1999).

Received: 1 November 2010. Accepted: 26 February 2011